Desalination 467 (2019) 257–262

Contents lists available at ScienceDirect

Desalination

journal homepage: www.elsevier.com/locate/desal

Desalination via chemical energy: An electrodialysis cell driven by spontaneous electrode reactions

S. Abu Khalla[a], M.E. Suss[a,b,*]

[a] Grand Technion Energy Program (GTEP), Technion – Israel Institute of Technology, Israel
[b] Faculty of Mechanical Engineering, Technion – Israel Institute of Technology, Israel

ABSTRACT

The form of the energy input for widely investigated desalination technologies include thermal energy (distillation), mechanical work (reverse osmosis) or electrical energy (electrodialysis and capacitive deionization). We here propose and characterize an electrodialysis-type desalination cell which is driven instead by spontaneous redox reactions occurring at electrodes. Thus, this system utilizes solely a chemical energy input to perform desalination, and requires no electricity input, instead producing electricity while desalinating. With our custom-built prototype system based on high performance zinc-bromine chemistry, we demonstrate the desalination of feedwater with an initial salinity of ~30 g/L while simultaneously generating up to 23.5 kWh of electricity per m^3 of desalted water. Further, we show our prototype cell can recover up to 85% of the input chemical energy as electricity during operation without needing a recovery device. The net energy usage, defined as chemical energy input minus electricity output, was measured to be 3.9 kWh/m^3 when desalting to near-zero concentration at 2 mA/cm^2 with our first-generation cell. Our proposed concept decouples reactant production from its usage in the cell, and we show that this decoupling can potentially lead to net negative operating costs when low-cost reactants are employed.

1. Introduction

Currently, the most utilized technology for water desalination is reverse osmosis (RO). Sea water RO plants deliver on the order of 10 million m^3 of treated water per day, via pressurizing the feedwater above its osmotic pressure of ~25 bar in order to drive water through a semi-permeable membrane that rejects salts [1,2]. As water scarcity increasingly affects more diverse locales [3], the requirements of a technological solution to combat scarcity are becoming more diverse, and technologies with novel functionalities should be explored. Many alternatives to RO have been investigated. Electrodialysis (ED) is an electrochemical system employing alternating anion and cation exchange membranes, and has been investigated for several decades as a desalination technology. In an ED cell, electricity is applied to drive electrochemical reactions at electrodes, and the resulting steady ionic current enables salt ion transport from a diluate channel into an adjacent brine channel. While ED cells are highly scalable and can desalinate at low (sub-osmotic) pressures, they are not as energy efficient as RO when performing sea water desalination [4]. In recent years, there has been a surge of interest in emerging electrochemical systems towards water desalination, such as capacitive deionization [5,6], desalination batteries [7–13], and desalination redox flow batteries [14,15]. Unlike ED, such systems are generally adapted from energy storage cells, and operate in a cyclic fashion by undergoing charge/discharge cycling. Generally, desalination occurs during cell charging, and during discharging brine is created and electrical energy can be recovered. Like energy storage systems, such cells are net users of electricity over a full charge/discharge cycle, although the electrical energy requirements for such systems have shown significant promise for brackish water desalination [12,16,25,26].

An alternative strategy is to develop desalination systems based on electrochemical cells performing continuous energy conversion rather than cyclic energy storage. The cell we propose and characterize here is shown schematically in Fig. 1a, and desalinates water by leveraging a chemical-to-electrical energy conversion process. Taken as a black box (Fig. 1a), our cell requires solely chemical energy as input and no electricity, and desalinates water while simultaneously producing electricity. As with an ED cell, our cell consists of one anion and one cation exchange membrane which sandwiches a desalination channel fed with feedwater. On the opposite side of the anion exchange membrane is an anode and anolyte, while a cathode and catholyte are placed opposite to the CEM. During operation, the reductant present in the anolyte (here Zn) and oxidant present in the catholyte (here Br_2) react spontaneously at the anode and cathode surfaces, respectively, providing an electric current between the anode and cathode which can be delivered to a load. The reductant and oxidant are carefully chosen to ensure they are electrostatically inhibited from entering the desalination channel by the AEM and CEM, respectively. The half-reactions also

* Corresponding author.
E-mail address: mesuss@technion.ac.il (M.E. Suss).

https://doi.org/10.1016/j.desal.2019.04.031
Received 3 February 2019; Received in revised form 21 April 2019; Accepted 27 April 2019
Available online 28 May 2019
0011-9164/

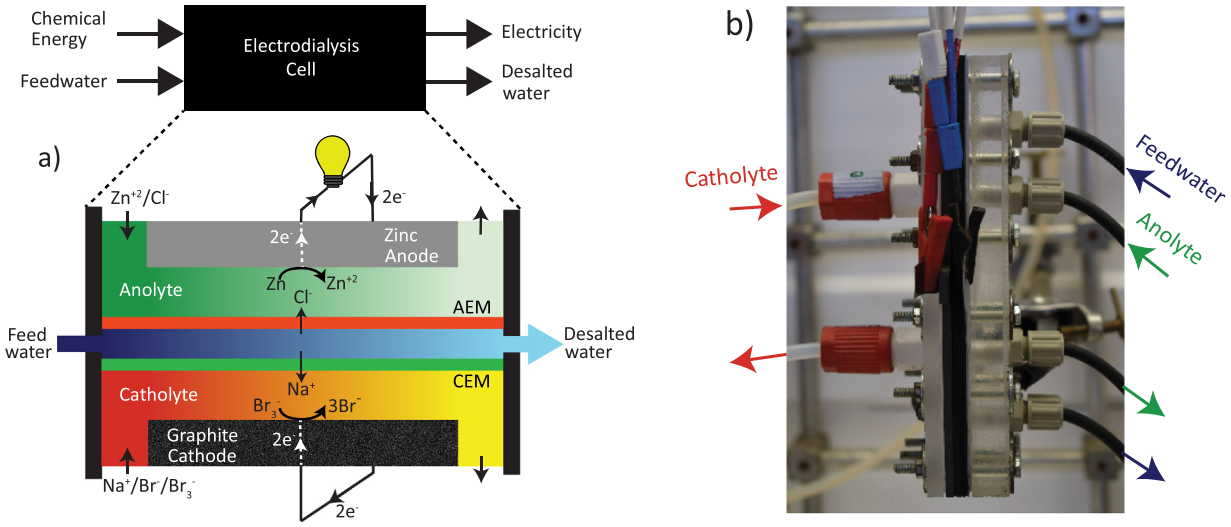

Fig. 1. a) Schematic illustrating the concept and working principle of the electrodialysis-type cell tested here. Taken as a black box, the cell requires only chemical energy as input, and outputs electricity while desalting water. Inside the black box, the cell undergoes spontaneous half-cell reactions at the zinc metal anode and bromine cathode, resulting in generated electricity. The spontaneous reactions drive an ionic current through the desalination channel, transporting sodium ions through a cation exchange membrane (CEM), and chloride ions through an anion exchange membrane (AEM). b) A picture of our custom-fabricated ED prototype with 10 cm^2 active area.

give rise to a spontaneous ionic current through the cell, which drives ion removal from the desalination channel. During operation, the feed is desalted as positively charged ions migrate from the desalination channel to the catholyte and negatively charged ions to the anolyte. The main differentiator from typical ED cells and the cell characterized here is that typical ED cells operate in electrolytic mode and thus require input electricity, but our cell operates in galvanic mode and delivers electricity. Compared to other emerging electrochemical desalination systems such as CDI and desalination batteries, which desalinate via two-stage charge/discharge processes and thus have limited salt storage capacity, our cell can instead be re-fueled, allowing for continuous desalination without interruption or capacity limitations.

We provide an experimental characterization of the desalination performance, electricity generation, and energy efficiency of our custom-built prototype cell based on high-performance Zn—Br_2 redox chemistry. When operated at 2 mA/cm^2 extracted current density, our cell demonstrates the near complete desalination of water with an initial salinity approximately that of sea water, while generating up to 23.5 kWh/m^3 of electricity while desalting. We show that our prototype cell can recover up to 85% of the input chemical energy as electricity during operation without needing a recovery device, and that the net energy usage, defined as chemical energy input minus electricity output, was as low as 3.9 kWh/m^3 when operated at 2 mA/cm^2. Desalination at higher currents is also demonstrated, up to 16 mA/cm^2, which allowed for significantly higher salt removal rates but at the cost of increased input chemical energy per m^3 desalted. For the ED concept developed here, we can decouple the production of the needed redox active chemicals from their use in the cell. We provide an analysis of the base operational costs and revenues for various potential redox chemistries, showing that driving such cells with low-cost chemistries can potentially lead to net negative operating costs.

2. Experimental methods

The custom-built prototype cell tested here is shown in Fig. 1b, and utilized zinc-bromine chemistry. Such a chemistry is considered to be high-performance because it allows for kinetically fast electrochemical reactions to minimize activation voltage losses at electrodes, and enables use of highly conductive electrolytes to minimize Ohmic voltage losses (around 100 mS/cm). Bromine (Br_2) and bromide (Br^-) complex to form negatively charged tribromide (Br_3^-), which is the dominant oxidant species [17,18]. Thus, such a chemistry is compatible with the cell concept shown in Fig. 1a, as the zinc ion transport is inhibited by the anion exchange membrane and Br^- and Br_3^- ions by the cation exchange membrane. While we here used zinc-bromine to achieve high desalination performance, numerous alternative chemistries are compatible, and in the future chemistries can be chosen with an emphasis on optimizing either desalination energy efficiency, operational costs, or safety and water quality (see Fig. 3c for an analysis based on operational cost). We made the anolyte by mixing zinc chloride salt into deionized water to form 1 L of 2 M $ZnCl_2$. For the catholyte, we mixed bromine and sodium bromide salt into deionized water to 1 L of 1 M Br_2/2 M NaBr. Thus, during operation of our ED cell, zinc metal was oxidized to zinc ions and tribromide ions reduced to bromide ions. The relatively large volume of anolyte and catholyte was chosen in order to maintain an approximately constant state of charge throughout a series of desalination experiments. The feedwater was prepared by adding NaCl to 30 mL of deionized water to create a 500 mM (29.22 g/L) NaCl solution.

The cell consisted of a custom-milled planar graphite cathode, 0.127 mm thick titanium sheet current collector at the cathode side and 0.62 mm thick zinc sheet for the anode (Alfa Aesar, United Kingdom), Viton rubber gaskets, and Neosepta ion exchange membranes (Neosepta AMX and CMX, Tokuyama, Japan). The endplates used were acrylic for the zinc side and PVDF for the bromine side. The anolyte and catholyte flow channels were made by cutting 6.7 by 1.5 cm channels into 1 mm thick Viton rubber gaskets, and stacking two gaskets per flow channel (flow channel thickness was 2 mm). Thus the active area of our cell used for current normalization was that of the anolyte and catholyte flow channels, which was 10 cm^2. The desalination channel was cut into a single 1 mm thick Viton rubber gasket with the channel dimensions of 12.5 by 1.5 cm. The desalination channel was longer than the anolyte and catholyte channels in order to allow for convenient injection and removal of the feedwater from the cell. The cell was sealed with fourteen M4, 48 mm long stainless steel bolts, which were plastic wrapped to prevent internal short circuiting. The connection to an external load was made through tabs on the titanium and zinc metal sheets.

All three flows, anolyte, catholyte and feedwater were recirculated through the cell using peristaltic pumps (Masterflex, Cole Parmer,

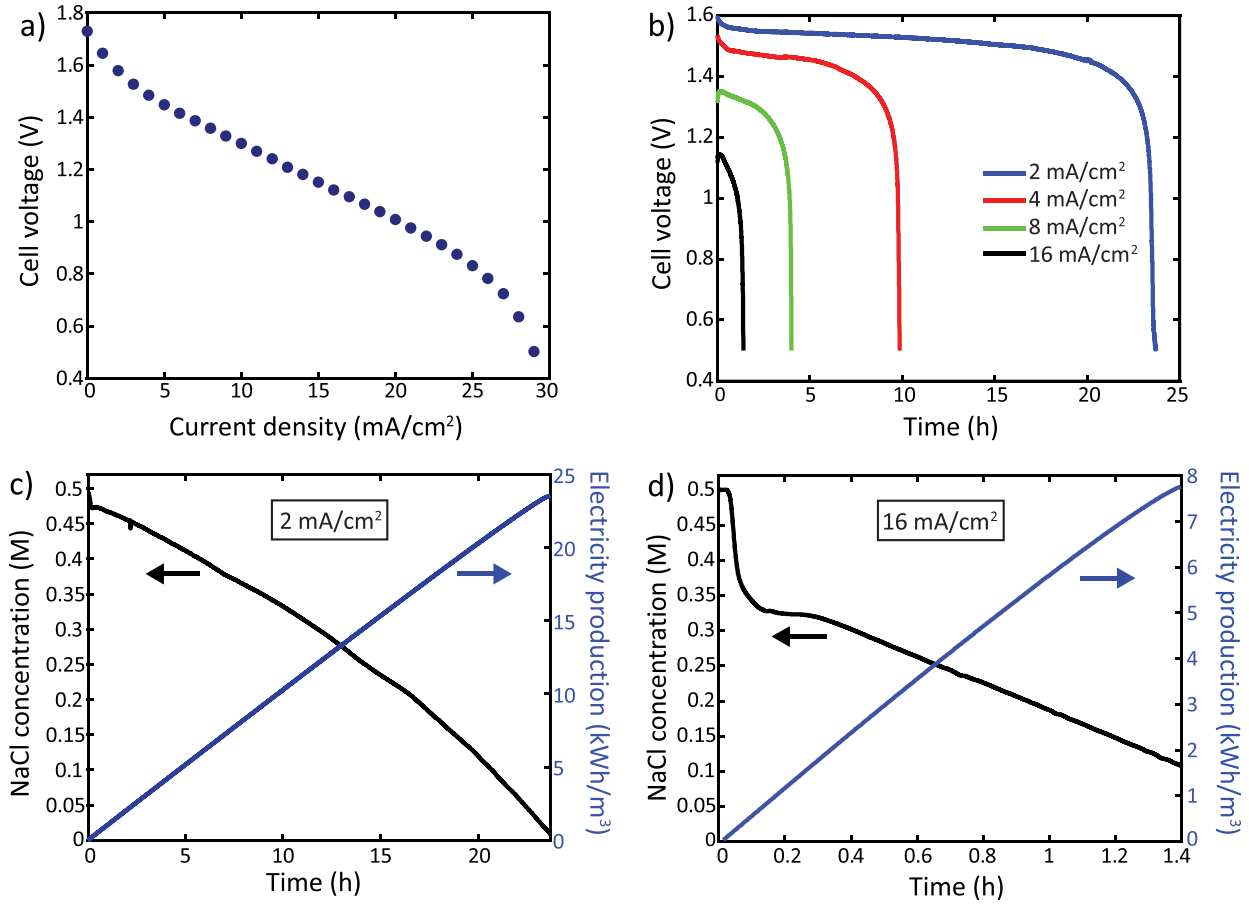

Fig. 2. a) A polarization curve showing measured equilibrium cell voltage of our ED cell versus extracted current. b) Measured cell voltage during constant current experiments at various currents from 2 to 16 mA/cm^2. c) Measured middle channel effluent concentration and cumulative electricity production by the cell during the experiment at 2 mA/cm^2 shown in b). d) Measured middle channel effluent concentration and cumulative electricity production during the experiment at 16 mA/cm^2 shown in b).

USA), at a flow rate of 0.5 mL/min for the feedwater, 1.5 mL/min for the anolyte, and 2 mL/min for the catholyte. During polarization curve measurements (Fig. 2a), a constant current was delivered from the cell to a potentiostat in steps of 1 mA/cm^2 (Biologic VSP, France), with a dwell time of at least 5 min per step to attain the equilibrium cell voltage. Also, for polarization curve measurements only, the feedwater volume used was 1 L instead of 30 mL to achieve a steady-state (constant salt concentration profile) in the desalination channel. For the constant current experiments (Fig. 2b–d), the ED cell delivered currents ranging from 2 to 16 mA/cm^2, while flow was maintained in all channels. During these experiments, we measured both the resulting cell voltage and the effluent conductivity leaving the desalination channel (Tracedec, Innovative Sensor Technologies GmbH, Austria). Conductivity was converted to NaCl concentration via a prepared calibration curve. Constant current experiments continued until cell voltage reached below 0.5 V, at which point the experiment ended.

3. Results and discussion

We here describe results of experiments performed with our prototype cell, shown schematically in Fig. 1a and pictured in Fig. 1b. In Fig. 2a, we show the obtained polarization curve, by plotting measured equilibrium cell voltage versus extracted current density. From this figure, we can observe that the cell's open circuit voltage (OCV) is measured to be about 1.74 V. A distinct activation region can be observed at lower currents, until about 5 mA/cm^2, after which a linear Ohmic region is observed until about 25 mA/cm^2. At higher currents, significant mass transport limitations are observed, with a limiting current at about 30 mA/cm^2. Such a limiting current density is roughly an order of magnitude lower than that predicted and observed for galvanic electrochemical cells with planar electrodes which are limited by bromine reduction (for similar bromine concentration) [18,19]. This suggests that the limiting current observed may not be due to reactant exhaustion at the cathode, but rather that salt concentration in the desalination channel approaches zero at the membrane surface. In Fig. 2b–d, we show results of constant current experiments. Fig. 2b shows the measured voltage from our cell when extracting currents from 2 to 16 mA/cm^2. As can be seen, setting a higher current resulted in a lower cell voltage, as is typical of fuel cell performance [20]. Each experiment was run until the cell voltage fell to 0.5 V, which was attained via rapid voltage decay at the end of all curves shown in Fig. 2b, a feature characteristic of a mass transport limitation. At the lower currents tested (2 and 4 mA/cm^2), a relatively stable cell voltage was obtained, where cell voltage decreases slowly as the middle channel is desalted. The relatively stable voltage lasts for several hours until the cell voltage suddenly drops (at ~24 h for 2 mA/cm^2 and ~10 h for 4 mA/cm^2). The sudden drop in cell voltage coincides with the near complete desalination of the middle channel, see Fig. 2c. When running the cell at the highest current of 16 mA/cm^2, the cell died roughly 1.5 h into the experiment, without reaching a stable voltage.

In Fig. 2c, we show the measured concentration of the effluent leaving the desalination channel of the cell, and the cumulative electricity produced by the cell during an experiment at an extracted current density of 2 mA/cm^2. The conductivity data was taken simultaneously to the voltage data of Fig. 2b. The initial concentration of the salty water pumped through the middle channel was 500 mM NaCl,

which is approximately the salinity level of seawater. At the start of the experiment, a quick reduction to ~470 mM is observed within the first 10 min, followed by slower and fairly steady salt removal as the salt water is recirculated through the desalination channel of the cell. Salt removal continued until the salt concentration reached about 10 mM at 24 h, at which point the cell voltage fell quickly to 0.5 V and the experiment ended (see Fig. 2b). Thus, the total salt concentration reduction was nearly two orders of magnitude during the 2 mA/cm^2 experiment. Electricity was produced by the cell during desalination, which can be calculated by the integral in time of cell voltage shown in Fig. 2b multiplied by the extracted current. In Fig. 2c, we show the cumulative electricity produced by the cell, which is roughly linear in time due to the near constant voltage of the cell during most of the experiment (Fig. 2b). The total electricity delivered by the cell during desalination was ~23.5 kWh/m^3 of desalted water. In Fig. 2d, we show the salt concentration and electricity produced for an extracted current of 16 mA/cm^2. Upon beginning the experiment, a distinct sharp drop in salt concentration to 350 mM is observed within about 10 min, similar to the initial transient seen at 2 mA/cm^2, but significantly stronger. After this initial transient, salt removal proceeds at a much faster rate relative to Fig. 2c, until the cell voltage suddenly drops to 0.5 V at about 1.4 h (Fig. 2b). As can be seen in Fig. 2d, the cell died before the middle channel was completely desalted, as at the end of the experiment the salt concentration was just above 100 mM. The latter points to a potentially important role of mass transport boundary layers in the desalination channel on the cell desalination performance. We hypothesize that while the bulk salt concentration was ~100 mM, the salt concentration adjacent to the membranes in the desalination channel approached zero [21], causing the observed sharp drop in cell voltage (Fig. 2b). Total electricity production during desalination at 16 mA/cm^2 was noticeably lower than for 2 mA/cm^2, and was ~7.8 kWh/m^3. Overall, the results of Figs. 2c and d demonstrate that the extracted current density must be carefully chosen if complete desalination is desired, and that there is a trade-off between electricity delivered during desalination and desalination rate (current density). Furthermore, Fig. 2d shows that our first-generation cell can attain order of magnitude higher desalination current densities relative to desalination batteries, which are thus far restricted to roughly 1 mA/cm^2 [9,10,12,22].

Fig. 2 showed the ability of our cell to deliver desalted water and electricity without requiring an electricity input. To analyze the potential of ED cells driven by spontaneous electrode reactions, we will develop a methodology to understand both its energy efficiency and cost proposition towards seawater desalination. In Fig. 3a, we show a schematic representation of the combined operation of our cell with a chemical production plant supplying the needed redox active chemicals. The main energy flows are the chemical energy input to the cell from the plant, $(kWh/m^3)_{chem}$, and the electrical energy output from the cell during desalination, $(kWh/m^3)_{elect}$, both per m^3 of desalted water. The chemical energy input to our cell can be calculated as the electricity it would have produced if the cell voltage had remained at OCV for the entire desalination process, and this process has the same duration as that shown in Fig. 2b. This input energy can also be interpreted as the electricity produced during a hypothetical lossless conversion of chemical-to-electrical energy (when there are no finite resistances in the ED cell). In our analysis, we neglect chemical energy losses due to reactant crossover through the membranes, as this loss mechanism is expected to be small relative to energy loss via resistive dissipation. We can then define an energy recovery efficiency as the ratio of the electricity output of the cell during desalination to the input chemical energy, $(kWh/m^3)_{elect}/(kWh/m^3)_{chem}$. In Fig. 3b, we plot the measured energy recovery efficiency, showing that the prototype cell can recover up to 85% of the input chemical energy as electricity when operated at 2 mA/cm^2, and thus at this current density 15% of the input energy was used to drive the desalination process. This recovery occurs without any dedicated energy recovery device (such as is needed in RO), as electricity is naturally outputted by the ED cell during operation. Recovery efficiency decreases with increasing current density, as is expected as higher currents represent further departures from equilibrium (from OCV), and drops to 60% at 16 mA/cm^2.

To gain additional insight, we can compare the energy used to drive desalination in our ED cell, $(kWh/m^3)_{chem}$ - $(kWh/m^3)_{elect}$, to the calculated thermodynamic minimum energy requirement for desalting a 500 mM NaCl feedwater, ΔG_{sep}. The energy used to drive desalination is measured to be 3.9 kWh/m^3 at 2 mA/cm^2, and increases with applied current to 5.2 kWh/m^3 at 16 mA/cm^2. The minimum energy, ΔG_{sep}, is calculated assuming a thermodynamically reversible separation process, and thus is unachievable in practice and independent of the technology used to perform the desalination. The calculation was performed using previously developed expressions for minimum energy [23], and using 1.5% water recovery, as this was the ratio of feedwater volume to the combined anolyte and catholyte volume in our prototype system. The calculated minimum thermodynamic energy ranges from ~0.33 to 0.63 kWh/m^3, because of the range of desalted water concentration achieved at the end of our desalination experiments (see Fig. 2c and d). We note that the latter calculation serves as an estimate of the minimum thermodynamic energy for our cell, as the process we performed was not solely a separation, but also we generated ionic species in the brine streams via spontaneous electrochemical reactions. The ratio of energy used to drive desalination to the calculated thermodynamic minimum energy is 6.3 at 2 mA/cm^2 (see Fig. 3b). Improved desalination efficiencies can undoubtedly be demonstrated in the future by undertaking optimization of the cell geometry and electrolyte chemistry to reduce major sources of resistance. The results shown here are in stark contrast to other electrochemical systems for water desalination, such as capacitive deionization, which are largely inefficient for seawater desalination and restricted to brackish water feeds [5].

In order to develop insight into the cost proposition of ED cells driven by spontaneous electrochemical reactions, we here provide an analysis of the basic operational costs and revenues of such cells. As shown schematically in Fig. 3a, the aspects we consider here are the cost of the reactants used to drive the cell, $(\$/m^3)_{chem}$, and the income from electricity produced by the cell, $(\$/m^3)_{elect}$. The estimated cost of a reactant per m^3 of seawater desalinated can be calculated as QMp/nF, where Q is the ionic charge in units of Coulombs per m^3 of feedwater, M is the reactant molar mass, F is Faraday's constant, n is the moles of electrons per mole of reactant, and p is the reactant price in units of \$/kg. In Fig. 3c, we show the calculated cost of reactants in units \$/m^3, for a feedwater of 0.5 M NaCl, and for various chemistries which are compatible with the concept (either as shown in Fig. 1a, or requiring three or four membranes). The total cost of reactants requires summing the cost per m^3 of both the reductant and oxidant used in the proposed cell. As can be seen in Fig. 3a, chemistries such as vanadium-iodine (V—I) and zinc-bromine (Zn—Br_2) are likely cost-prohibitive for use in large-scale water desalination. This is because their reactant cost alone is on the order of \$10^2-10^3/m^3, whereas for seawater desalination by RO, the total cost of the desalted water is typically between \$0.5/m^3 - \$1/m^3 (of which ~35% is the cost of electricity required during operation) [2,24]. Other chemistries, namely those utilizing low-cost sulfur, hydrogen, or iron, and those that are air-breathing, demonstrate promising cost propositions, with reactant cost achieving on the order of \$1/m^3. To gain further insight, the revenue resulting from the generated electricity during cell operation should be subtracted from the reactant costs. As shown in Fig. 2c, when desalting seawater with our prototype cell at 2 mA/cm^2, we generate 23.5 kWh/m^3. Thus, assuming the sale of electricity at \$0.15/kWh, our ED cell provides up to ~\$3.5/m^3 of revenue (dashed line in Fig. 3c). This value of revenue is specific to our first-generation prototype Zn—Br_2 cell, while future cells optimized for minimal resistive losses should be able to achieve similar revenues at greater than 2 mA/cm^2 current densities, enabling higher desalted water throughput. Thus, the cost analysis proposed here

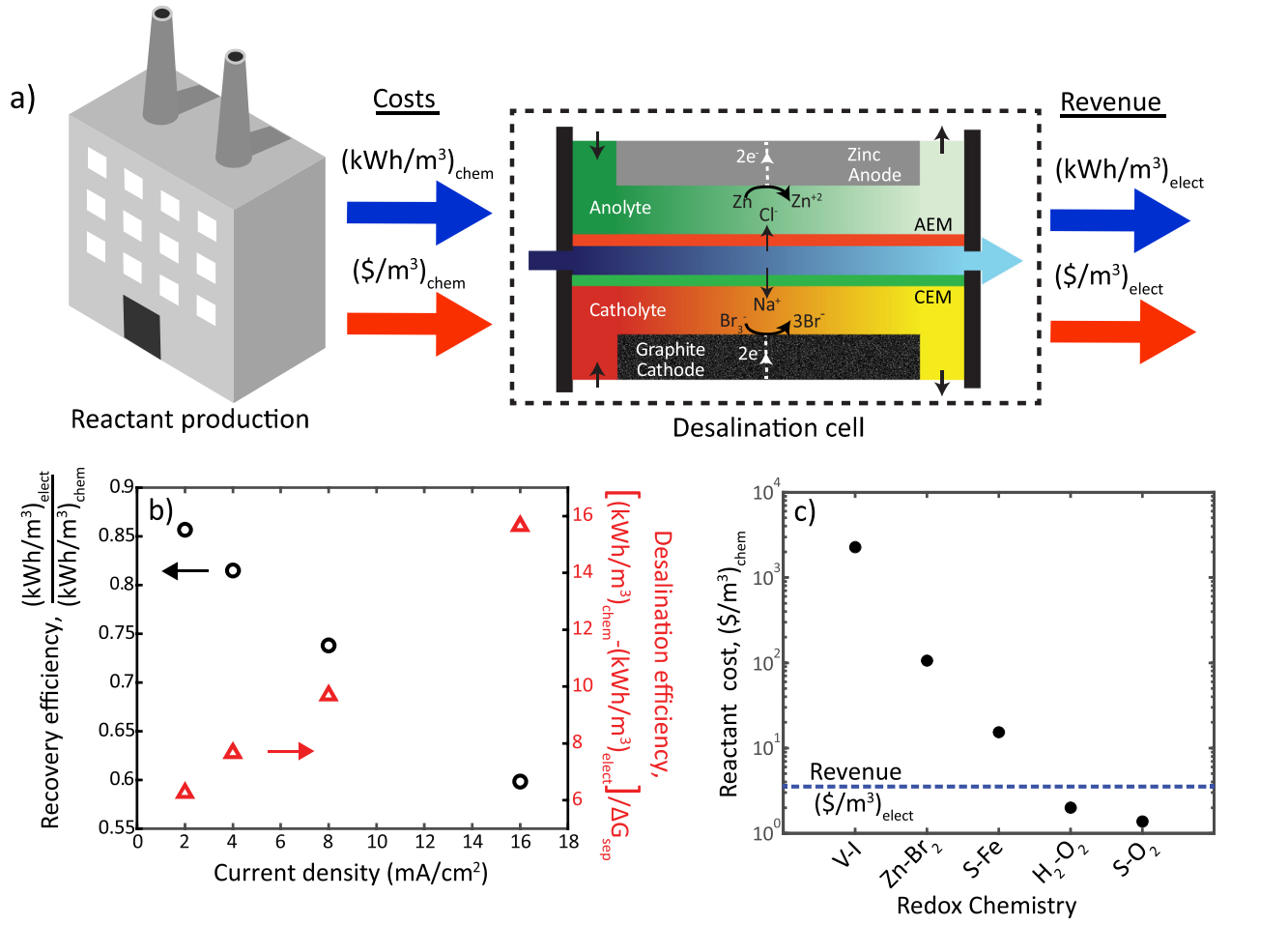

Fig. 3. a) Schematic of the energy and monetary inputs and outputs for an ED cell driven by spontaneous electrochemical reactions, with units of kWh or $ per m^3 of desalted seawater. The proposed cell utilizes reactants produced at minimized cost in a separate facility, thus decoupling reactant production from its usage in the cell. b) Measured energy recovery efficiency (left axis, black circles) and desalination efficiency (right axis, red triangles) versus extracted current density, obtained with our prototype. c) Evaluation of the cost of potential reactants for the ED cell, in units of $ per m^3 of desalted seawater. The dashed line shows the calculated revenue from the electricity production of our prototype cell.

suggests that by decoupling reactant production and its usage in the cell, as shown in Fig. 3a, it may be possible to desalt water with a net negative operational cost per m^3. This may occur if the active chemicals come at zero cost (e.g. O_2 from air), or are produced inexpensively as a by-product from common chemical processes (e.g. S), so that the revenue from generated electricity surpasses the cost of the reactants needed. Note that if we instead generated the reactants in the cell electrochemically, obtaining net negative operating costs would not be possible, as such production would necessarily require higher electrical input to the cell than the electricity gained on discharge [14,15]. There remain many future steps towards conclusively demonstrating exceptionally low, or even negative, operational costs for such a cell, including incorporating the cost of fouling protection, upstream filtration, anode replacement for metal-based chemistries, and disposal of the spent anolyte and catholyte streams. Nevertheless, the base cost analysis provided here demonstrates that developing ED cells based on low-cost reactants has the potential to lead to ultra-low cost desalted water.

4. Conclusion

We here characterized experimentally an electrodialysis cell which takes solely chemical energy as input in the form of Zn and Br_2 reactants, and outputs desalted water and electricity. With our custom-fabricated prototype, we demonstrated electricity production of 23.5 kWh/m^3 of desalted water while desalinating a feed of ~30 g/L NaCl to near-zero concentration at 2 mA/cm^2 extracted current. We further provided an analysis of base operational costs, which demonstrates that by decoupling reactant production and use as well as using low-cost reactants, such ED cells can potentially yield net-negative operational costs. Future studies should focus on understanding and improving such cell performance with low-cost reactants, and propose and test scale-up strategies.

Acknowledgements

This study is supported by The Nancy and Stephen Grand Technion Energy Program (GTEP), and the Ministry of National Infrastructures, Energy and Water Resources via the undergraduate to graduate student scholarships in the energy fields. The authors would like to acknowledge funding from the Israel Science Foundation in the framework of the Israel National Research Center for Electrochemical Propulsion (INREP) project.

Declaration of competing interest

There are no conflicts to declare.

References

[1] M. Elimelech, W.A. Phillip, Science 333 (2011) 712–717.
[2] N. Ghaffour, T.M. Missimer, G.L. Amy, Desalination 309 (2015) 197–207.
[3] A.Y. Hoekstra, M.M. Mekonnen, A.K. Chapagain, R.E. Mathews, B.D. Richter, PLoS One 7 (2012).
[4] H. Strathmann, Desalination 264 (2010) 268–288.
[5] M. Suss, S. Porada, X. Sun, M. Biesheuvel, J. Yoon, V. Presser, Energy Environ. Sci. 8 (2015) 2296–2319.
[6] S. Porada, R. Zhao, A. Van Der Wal, V. Presser, P.M. Biesheuvel, Prog. Mater. Sci. 58 (2013) 1388–1442.
[7] M.E. Suss, V. Presser, Joule 2 (2018) 10–15.
[8] M. Pasta, C.D. Wessells, Y. Cui, F. La Mantia, Nano Lett. 12 (2012) 23–27.
[9] S. Porada, A. Shrivastava, P. Bukowska, P.M. Biesheuvel, K.C. Smith, Electrochim. Acta 255 (2017) 369–378.
[10] D. Nam, K. Choi, J. Am. Chem. Soc. 139 (2017) 11055–11063.
[11] P. Srimuk, F. Kaasik, B. Krüner, A. Tolosa, S. Fleischmann, N. Jäckel, M.C. Tekeli, M. Aslan, M. Suss, V. Presser, J. Mater. Chem. A 4 (2016) 18265–18271.
[12] T. Kim, C.A. Gorski, B.E. Logan, Environ. Sci. Technol. Lett. 4 (2017) 444–449.
[13] J. Lee, P. Srimuk, S. Carpier, J. Choi, ChemSusChem 11 (2018) 3460–3472.
[14] D. Desai, E.S. Beh, S. Sahu, V. Vedharathinam, Q. Van Overmeere, C.F. De Lannoy, A.P. Jose, A.R. Völkel, J.B. Rivest, ACS Energy Lett. 3 (2018) 375–379.
[15] S.H. Xianhua Hou, Qian Liang, Hu Xiaoqiao, Yu Zhou, Ru Qiang, Fuming Chen, Nanoscale 10 (2018) 12308–12314.
[16] R. Zhao, S. Porada, P.M. Biesheuvel, A. Van der Wal, Desalination 330 (2013) 35–41.
[17] M.E. Suss, K.M. Conforti, L. Gilson, C.R. Buie, M.Z. Bazant, RSC Adv. 6 (2016) 100209–100213.
[18] R. Ronen, I. Atlas, M. Suss, J. Electrochem. Soc. 165 (2018) A3820–A3827.
[19] W.A. Braff, M.Z. Bazant, C.R. Buie, Nat. Commun. 4 (2014) 2346.
[20] R. O'hayre, S.-W. Cha, F.B. Prinz, W. Colella, Fuel Cell Fundamentals, John Wiley & Sons, 2016.
[21] M. Tedesco, H.V.M. Hamelers, P.M. Biesheuvel, J. Memb. Sci. 510 (2016) 370–381.
[22] J. Lee, S. Kim, J. Yoon, ACS Omega 2 (2017) 1653–1659.
[23] N.Y. Yip, M. Elimelech, Environ. Sci. Technol. 46 (2012) 5230–5239.
[24] M.K. Wittholz, B.K.O. Neill, C.B. Colby, D. Lewis, Desalination 229 (2008) 10–20.
[25] Ashwin Ramachandran, et al., High water recovery and improved thermodynamic efficiency for capacitive deionization using variable flowrate operation, Water research 155 (2019) 76–85.
[26] L. Wang, J. Dykstra, S. Lin, Energy Efficiency of Capacitive Deionization, Environ. Sci. Technol. (2019).